


Oral Targeted Delivery of *Codonopsis Radix* Polysaccharide via Succinyl -DHA Functionalized Nanoparticles Efficiently Alleviates Ulcerative Colitis

Kang Dong^{1,*}, Xin Wang^{1-3,*}, Ze-jia Zhou¹⁻³, Xin-ru Zheng¹⁻³, Zhuang-peng Chang¹, Rui Zhao^{1,2}, Jun-jin Liu¹⁻³, Rui-gang Hou¹⁻³, Xiao Zhang¹⁻³, Yun-yun Shao¹⁻³

¹Department of Pharmacy, Second Hospital of Shanxi Medical University, Taiyuan, Shanxi, People's Republic of China; ²School of Pharmacy, Shanxi Medical University, Taiyuan, Shanxi, People's Republic of China; ³Medicinal Basic Research Innovation Center of Chronic Kidney Disease, Ministry of Education, Shanxi Medical University, Taiyuan, People's Republic of China

*These authors contributed equally to this work

Correspondence: Yun-yun Shao; Rui-gang Hou, Department of Pharmacy, Second Hospital of Shanxi Medical University, Taiyuan, Shanxi, People's Republic of China, Tel +86 351-3365405, Email shaoyunyun4466@163.com; ruiganghou9966@163.com

Introduction: Ulcerative colitis (UC) is a chronic intestinal disease characterized by spleen-lung qi deficiency and dampness-pathogenic obstruction. Although there are various treatment options available, patients frequently encounter significant drug-related side effects. Previous studies have shown the potential of *Codonopsis Radix polysaccharides* A (CPA) in treating UC, but their limited bioavailability has restricted their clinical use. Therefore, the objective of this study was to develop a novel formulation that can address the aforementioned limitations and assess its potential advantages.

Methods and Results: We synthesized a negatively charged amphipathic prodrug called CPA-SA-DHA (CSD), which consists of CPA as the hydrophilic component, and succinic anhydride and docosahexaenoic acid as the hydrophobic segments. The CSD nanoparticles obtained had a particle size of 180.0 ± 3.2 nm, a negative zeta potential of -29.8 ± 5.3 mV, and a uniform shape with a PDI index of 0.230 ± 0.003 . The interaction between positive and negative charges significantly increased the retention time of CSD nanoparticles in the colonic microenvironment. Furthermore, CSD nanoparticles demonstrated enhanced bioavailability in UC mice compared to CPA. Additionally, we observed that CSD nanoparticles exhibited therapeutic effects on DSS-induced UC mice by regulating the diversity and abundance of gut microbiota. This effect may be mediated by the inhibition of pro-inflammatory signaling pathways TLR4/NF- κ B.

Conclusion: These findings confirm the potential of CSD nanoparticles as a promising treatment option for UC.

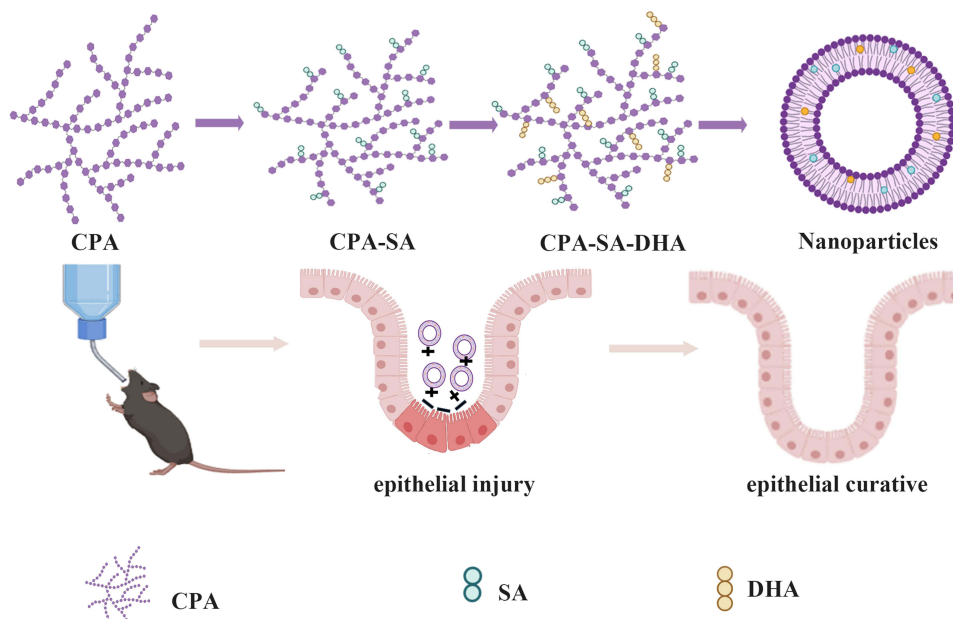
Keywords: ulcerative colitis, *Codonopsis Radix* polysaccharide, succinic acid, docosahexaenoic acid, nanoparticles

Introduction

Ulcerative colitis (UC) is a subtype of inflammatory bowel disease. Its main clinical symptoms are abdominal pain, fecal blood, weight loss, and diarrhea.^{1,2} UC is characterized by damage to the colonic mucosal barrier, which leads to increased permeability of the epithelial barrier.³ In recent years, there has been an increase in the mortality and morbidity rates of UC, particularly among young people. The most commonly used medications for UC therapy are anti-inflammatory drugs (such as 5-aminosalicylic acid and corticosteroids) and agents that repair the mucous barrier (such as azathioprine, 6-mercaptopurine, and tacrolimus).⁴⁻⁶ However, these drugs have several limitations, including inefficacy, ineffective control of drug release, and limited targeting of inflamed areas.⁷ Given these limitations, researchers are now looking for new therapeutic agents that can cure or alleviate the symptoms of UC.

In the last decade, there has been a growing interest in traditional Chinese medicine (TCM) among researchers. This is largely due to the presence of numerous active ingredients found in TCM, including polysaccharides, saponins, flavonoids,

Graphical Abstract



polyphenols, and polypeptides.³ These active compounds have become an important source for developing new drugs.^{8,9} Polysaccharides, in particular, are considered one of the main active ingredients in TCM and possess a range of biological activities such as immunoregulatory, antioxidant, antiviral, and anti-tumor effects.¹⁰ Nowadays, they have become a very important index for evaluating the quality of TCM. *Codonopsis Radix* is derived from the root of *Codonopsis pilosula* (Franch.) and has long been used in traditional Chinese medicine for replenishing healthy qi, nourishing blood, and promoting the generation of bodily fluids.^{11,12} In our previous studies, an inulin-type fructan called *Codonopsis Radix* polysaccharide A (CPA) was extracted from “Lu-dang” (produced in Changzhi of Shanxi Province). The structure of CPA is a (2→1)-β-D-fructofuranose oligosaccharide with a molecular weight of 3.6 KDa. It has been shown to be effective in treating DSS-induced colitis and can be a potential new drug candidate derived from plants.^{13,14}

Given that the high failure rate of new drug research due to pharmacokinetics, it was crucial to investigate the pharmacokinetics profile and cytotoxicity mechanism of CPA. However, it is extremely difficult to detect the concentrations of polysaccharides using conventional detectors due to their complex chemical structure and the lack of UV absorption or fluorescent groups.¹⁵ Currently, the two most commonly used methods for quantitatively determining polysaccharides are radioactive element labeling and fluorescence labeling.¹⁶ Fluorescence labeling technology involves converting polysaccharide molecules into polysaccharide-fluorescent macromolecules through covalent derivatization or physical adsorption.¹⁷ This transformation allows for quantitative detection by giving the polysaccharide molecules fluorescence characteristics. In our previous study, we utilized a fluorescence labeling technique to create a fluorescent derivative of CPA called FCPA.¹³ Subsequently, we examined the in vivo behavior of FCPA. The pharmacokinetic findings revealed that FCPA exhibits a brief duration within the body and is rapidly metabolized by gut microbiota following oral administration, thus leading to low bioavailability. The results also showed that the absolute bioavailability of CPA after oral administration was extremely low (3.49%). Moreover, only a small fraction of CPA (with an apparent permeability coefficient $P_{app} < 1 \times 10^{-6} \text{ cm S}^{-1}$) could enter Caco-2 cells through non-clathrin and alveolin-dependent endocytosis pathways.^{13,15} Therefore, it is highly desirable to develop a new formulation that can overcome these limitations. This will facilitate the development of novel drugs based on CPA.

In drug delivery, nanoparticles (Nps) are a new type of preparation that possess small size, strong drug loading ability, and a multi-functional surface structure.^{18,19} They offer significant advantages in addressing the limitations of active ingredients

in TCM for treating UC, such as their hydrophobic nature, poor permeability and oral stability, and low bioavailability. For instance, Yao-Xing Dou et al demonstrated that by preparing bluesin D into Nps, its water solubility and bioavailability can be improved.²⁰ Haiting Xu et al wrapped curcumin in chitosan/alginate hydrogel to create Nps, which can target giant cells in the colon and extend the duration curcumin remains in the body.²¹ Nps can permeate the entire intestinal mucosa and accumulate in the colitis tissue due to their suitable particle size range of 100~1000 nm, thus avoiding rapid elimination through diarrhea.²² Moreover, Nps can specifically deliver drugs to the lesion site through the “enhanced permeability and retention effect (EPR)”, thereby enhancing drug absorption by activated immune cell.²³ However, the therapeutic effect of Nps is still unsatisfactory due to this passive targeting. By modifying the surface of Nps, their specific cell-targeting functions can be enhanced, leading to increased drug accumulation at the colitis site.²⁴ Therefore, active targeting mode of Nps has become an effective treatment for UC. The colonic mucosa of patients with UC is characterized by defects in the intestinal mucosa, leading to a loss of barrier function and increased epithelial permeability. Although these defective mucous membranes only make up 1% of the surface area of the intestinal mucosa, there is a significant increase in the concentration of positively charged proteins.²⁵ This increase facilitates the accumulation of negatively charged Nps in the damaged mucosal areas, thereby enabling them to target areas of inflammation in the colon.

Therefore, in this study we developed a negatively charged Nps based on CPA. Firstly, CPA was modified into a negatively charged conjugate by succinic anhydride (SA, which was called CPA-SA. However, SA has a small molecular weight, too much succinic anhydride may destroy the biological activity of CPA. Therefore, another hydrophobic substance was introduced to lower the amount of SA. Considering the well hydrophobicity and bioactivity, docosahexaenoic acid (DHA) was applied to modify CPA-SA. Thus, the prodrug consists of CPA as the hydrophilic part, and succinic anhydride and DHA as the hydrophobic segment was developed. To confirm the structure, we conducted infrared chromatography and ¹HNMR analyses. The Nps were prepared using the ultrasonic method. The morphology of CSD was observed through TEM and DLS. Finally, we assessed the therapeutic effects of CPA, CPA-SA-DHA, and CSD nanoparticles in LPS-induced NCM cells and UC mice.

Materials and Methods

Dextran Sulfate Sodium Salt was purchased from MP Biomedicals (Canada), while Sephadex G-25 medium was obtained from Solarbio Science & Technology Co., Ltd. (Beijing, China). Docosahexaenoic Acid (DHA) and Succinic anhydride (SA) were provided by Macklin Biochemical Co., Ltd (Shanghai, China). 1-(3-dimethylaminopropyl)-3-ethylcarbodiimide hydrochloride (EDC) and N-hydroxysuccinimide (NHS) were obtained from Aladdin Chemical Co. (Shanghai, China), and Mesalamine (SASP) was provided by Energy Chemical (Anhui, China). Lipopolysaccharide (LPS) and Myeloperoxidase (MPO) were purchased from MedChemExpress (USA), while Cell Counting Kit 8 (CCK8) was obtained from Dojindo (Japan). The NCM460 cell line was purchased from Procell Life Science & Technology Co., Ltd. (Wuhan, China). Minimum Essential Medium (MEM), Fetal Bovine Serum (FBS), penicillin-streptomycin, and 0.25% Trypsin-EDTA solution were obtained from Gibco (USA).

Extraction and Purification of CPA

CPA was acquired based on previous studies.²⁶ The roots of *Codonopsis pilosula* were soaked and extracted three times with deionized water (1:20, w/v) at room temperature. The filtrate was combined and subjected to centrifugation. The resulting filtrate was then concentrated to 1/4 of its original volume using a rotary evaporator. Next, it was precipitated with a 95% ethanol solution and left overnight at 4 °C. The total polysaccharide was obtained after washing with anhydrous ethanol, acetone, and petroleum ether, respectively. To purify the total polysaccharide and obtain a homogeneous polysaccharide (CPA), the total polysaccharide solution was filtered through membranes of grades 100,000, 8000, 5000, and 3000 using a TFT ultrafiltration device (Millipore Corporation, Billerica, MA, USA). Finally, CPA was obtained by freeze-drying the filtrate.

Synthesis of CPA-SA (CS) and CPA-SA-DHA (CSD)

The CS conjugate was prepared using a previously reported method.²⁷ Firstly, 300 mg of CPA was dissolved in 10 mL of deionized water. The pH was then adjusted to 9.0 using 10% NaOH. Separately, 50 mg of SA was dissolved in 2 mL of

deionized water. Next, the SA solution was slowly added to the CPA solution while stirring magnetically at 40 °C and 500 r/min. The mixture was left to react for 4 hours at 40 °C. Once the reaction was complete, hydrochloric acid was added to adjust the pH to 7.0. The mixture was then dialyzed and freeze-dried to obtain CS powder.

To synthesize CSD conjugate, CS solution was obtained by dissolving 300 mg of CS in 6 mL DMSO. 43.2 mg NHS and 71.9 mg EDC were added to the DHA solution and reacted at room temperature for 2 h. Then the mixture was slowly added to CS solution and reacted at room temperature for 48 h. After the reaction was completed, 10% NaOH was applied to adjust the pH to 7.0. The mixture was dialyzed and freeze-dried to yield CSD powder. The dried CSD powder was evenly ground in a mortar with an appropriate amount of potassium bromide, then pressed into thin slices using an infrared tablet press. The infrared spectrum was obtained with a Fourier transform infrared spectrometer (FTIR).

Preparation of CSD Nps Powder

CSD/FITC+ CSD (FCSD) was dissolved in DMSO to prepare a 10 mg/mL stock solution. Then 10 μ L stock solution was added drop-wise into 1 mL deionized water under the condition with ultrasonic vibration (100 W, 26 h) for 10 min. CSD Nps were generated by hydrophilic-lipophilic interactions-driven self-assembly. Finally, the CSD Nps was dialyzed and freeze-dried to yield CSD Nps powder.

The Characterization of CSD Nps

The freshly prepared nanoparticles were dissolved in water and sonicated for 5 minutes. A 5 μ L sample solution was placed onto a copper grid and covered with an ultra-thin carbon film for 5 minutes. After removing the excess liquid, the sample was dried at room temperature. The morphology was observed using a Transmission Electron Microscope (TEM) with an accelerated voltage of 200 kV.

The prepared sample solution was appropriately diluted, then 1 mL of the solution was drawn into the sample pool to measure the nanoparticles' potential using dynamic light scattering (DLS).

Stability of CSD Nps in vitro

The stability of CSD Nps was assessed by analyzing alterations in particle size when exposed to artificial gastric juice and artificial intestinal juice for various durations (0~6 h). Specifically, 50 mg of Nps was dissolved in 500 mL of artificial gastric juice at a pH of 2.00 ± 0.20 and artificial intestinal juice with at a pH of 6.80 ± 0.20 . Subsequently, the particle size of the nanoparticles was then measured using DLS after different incubation times (0, 1, 2, 4, 6 h).

Cell Culture

The human colon epithelial cells NCM460 are cultured in DMEM medium (Gibco™) containing 10% fetal bovine serum and penicillin-streptomycin solution. The cell lines were cultured under 5% CO₂ and 90% relative humidity. The culture medium was replaced every 2 d. When the cells became 80% to 90% confluent, they were passaged and frozen for storage. The activation of inflammation in NCM460 cells was triggered with LPS.

In vitro Cytotoxicity Assay

NCM460 cells were seeded onto 6-well plates with a density of 10^4 cells/well and cultured for 24 h. Then the cells were treated with various concentrations (50, 100, 200, 400, 800, 1600 and 3200 μ g/mL) of CSD Nps, respectively. After incubation for 24 h, the cells in each well was substituted with 200 μ L of CCK8 solution for 2 h at 37 °C. The absorbance at 570 nm was recorded using a microplate reader.

In vitro Anti-Inflammation Efficacy

To simulate the inflammatory micro-environment in vitro, NCM460 cells were incubated with LPS at the concentrations of 20 μ g/mL. After intervention, inflammatory model was evaluated by the mRNA level of IL-6. To evaluate the intervention effect of CSD Nps, the cultured cells were divided into the following groups: LPS induced group, CPA group, CPA+SA+DHA mixture (CSD Mix) group and CSD Nps group. The four groups of cells were collected to extract total RNA by Trizol reagent. Total RNA from NCM460 cells was isolated by M5 Universal Plus RNA Mini Kit. The

purity and concentration of RNA were evaluated by measuring the ratio of absorbance at 260/280 nm by spectrometry. 500 ng of RNA was added to the working solution of reverse transcription system kit (Super plus qPCR RT kit) to synthesize cDNA following the manufacturer's instructions. Real-time PCR reaction in 20 μ L-sized reactions was performed using the SYBR Green Master mix PCR kit on 7500 AB-Step one real-time PCR System (Applied Biosystems, Carlsbad, CA, USA). The experimental data were normalized by that of GAPDH and analyzed by the $2^{-\Delta\Delta C_t}$ method.

Animals

C57BL/6 mice were purchased from Si Pei Fu Beijing Biotechnology Co., Ltd. Mice were housed in specific pathogen-free conditions with free access to water and food. All experiments involving mice were approved by Committee on Use of Human and Animal Subjects in Teaching and Research of the Second Hospital of Shanxi Medical University (DK2023040). The entire procedure of animal work was performed in compliance with the basic ethical principles of animal experiments and the 3R principles.

DSS-Induced Colitis Model

C57BL/6 mice were used in this experiment to induce UC mice. They were randomly divided into seven groups (n=10 per group), including a normal group, 3% DSS group, SASP group (positive drug, 200 mg kg⁻¹ for 10 days), CSD Mix group (112 mg kg⁻¹ for 10 days), 3% DSS+CSD nanoparticles-low dose group (28 mg kg⁻¹ for 10 days), 3% DSS+CSD nanoparticles-median dose group (56 mg kg⁻¹ for 10 days), 3% DSS +CSD nanoparticles-high dose group (112 mg kg⁻¹ for 10 days). To develop a colitis model, we administered mice with 3% DSS (36–50 kDa; MP Biomedicals) in their drinking water from day 1 to day 7. From day 8 to day 10, we replaced the DSS solution with regular drinking water for the control and UC mice groups. For the CSD mixture group, we orally administered the mice with a CSD mix solution. In the CSD nanoparticles-median dose group, we administered the mice with different dosages of CSD Nps. During this period, body weight, feces and gross bleeding of mice were measured to monitor the colitis progression and calculate the disease activity index (DAI). On the tenth day, mice were sacrificed by cervical dislocation, tissues were collected and then stored at -80 °C until analysis. Colon length was measured and gently washed with physiological saline. Then the entire colon was collected for further analysis, three pieces of distal section were used for histological assessment. The remaining colon tissue samples were used for determining the concentrations of cytokines. Feces were collected for microbiome analysis.

Pharmacokinetics Studies of CSD Nps

Pharmacokinetic studies are performed to evaluate the bioavailability of CSD Nps in UC mice for 24 hours. UC mice were fasted for 12 h before experiment. For determining the concentration of CSD, the near-infrared dye FITC was loaded as a fluorescence probe in Nps. Our previous studies showed that 56 mg kg⁻¹ CPA was effective in alleviating DSS-induced colitis. Therefore, FITC labeled nanoparticles FCSD was orally administrated to the UC mice at the dose of 56 mg kg⁻¹. Approximately 0.5 mL blood samples were collected by removing the eyeballs of mice at the setting times of 60, 120, 240, 360, 720 and 1440 min. All blood samples were collected in heparinized eppendorf tubes and centrifuged at 4000 rpm for 10 minutes. Plasma was collected and stored at -80 °C until analysis.²⁸ The DAS (Drug and Statistics) software (version 3.0, Mathematical Pharmacology Professional Committee of China, Shanghai, China) was used to calculate the pharmacokinetic parameters.

Microbiota 16S rRNA Gene Sequencing

The total microbial DNA was extracted by DNeasy-PowerSoil Kit (Qiagen, Dusseldorf, Germany) according to the manufacturer's instructions. After assessing the concentration and integrity of DNA, the DNA was diluted to amplify the V4 hypervariable region of the 16S rRNA gene. To assess the difference in gut microbiota compositions of different groups, alpha diversity indexes were estimated using Chao 1 and Shannon. Chao1 is an index of the bacterial species and Shannon indices represent microbial diversity. The raw data files were quality-filtered by FASTP (version 0.20.0).

Operational taxonomic units (OTUs) were used to cluster the sequences based on 97% similarity. Each OTU representative sequence was analyzed with RDP Classifier (version 2.2).

Quantitative Real-Time PCR

RT-qPCR was carried out according to the manufacturers' instructions. Briefly, total RNA of colon tissue was extracted using the M5 hiPer Total RNA Extraction Reagent (Mei5 Biotechnology Co., Ltd, China). cDNA was synthesized from the extracted RNA using M5 Super qPCR RT Kit with gDNA remover (Mei5 Biotechnology Co., Ltd, China). Reverse transcription was performed using SYBR Green qPCR Kits. The mRNA expressions of target genes were calculated using GAPDH as a reference gene. The primer sequences of TLR4, PI3K, AKT, p65 and GAPDH were listed in Table 1.

Western Blot Analysis

Western blot analysis was carried out to evaluate the protein expression levels of TLR4/NF- κ B signal pathway. Briefly, protein samples were extracted from colon tissues of different groups and the protein concentrations was assayed by BCA Protein Assay. Subsequently, the protein samples were transferred to polyvinylidene fluoride membranes (Solarbio, China), where they were blocked with 5% nonfat milk for 0.5 h and then probed with the corresponding primary antibodies (anti-TLR4, 1:1000; anti-AKT/P-AKT, 1:1000; anti-P65/P-P65, 1:1000; anti-PI3K/P-PI3K, 1:1000; AB Clonal Biotechnology, WuHan, China) overnight at 4°C. Subsequently, the membranes were incubated with HRP-labeled secondary antibodies (1:1500, Zhongshan Jinqiao Biotechnology Co., Ltd, Beijing, China) for 1 h. The blots were visualized by enhanced chemiluminescence reagents with GAPDH (1:4000, Hangzhou Xiezi Biotechnology Co., Ltd, Hangzhou, China) as the internal control. The immunoreactive signals were observed using Alphaview and ImageJ software.

Statistical Analysis

All the results were repeated at least three times. All data in the chart and text were expressed as mean \pm standard error. Statistical analysis was executed by GraphPad Prism (v6.0, La Jolla, CA, USA). *T*-test was used to compare the differences between two groups. For multiple comparisons, all data was analyzed using univariate ANOVA. *P*-values <0.05 were considered significant.

Results and Discussion

Synthesis and Characterization of CSD Conjugate

In this study, the CSD conjugate was synthesized through a direct esterifying reaction of CPA, SA, and DHA (Figure 1). Different grafting degrees of SA and DHA were achieved by adjusting the amount of CPA, SA, and DHA as shown in Table 2. Next, we selected the appropriate grafting degree based on the state of the CSD conjugate. To confirm the synthesis of the conjugate, we conducted ¹H NMR and FTIR analyses. We dissolved CPA, SA, CPA-SA, and CSD in deuterium water (D₂O), while DHA was dissolved in deuterated chloroform (CDCl₃). Figure 2A presents the FTIR spectra of CPA, SA, DHA, CPA-SA, and CSD. The signals at 1219 cm⁻¹ and 1132 cm⁻¹ correspond to the C-O-C stretching vibration absorption in CPA-SA and CPA-SA-DHA. Additionally, the signal at 1737.86 cm⁻¹ is attributed to the C=O stretching vibration absorption peak formed by the dehydration of the hydroxyl groups in DHA and CPA. There is a small peak at 3013.27 cm⁻¹, which is the stretching vibration peak of =C-H in DHA. The results indicated that the synthesis of CPA-SA and CPA-SA-DHA was successful.

Table 1 Sequences of Primers Used for PCR

Gene	Forward Primer (5'-3')	Reverse Primer (3'-5')
TLR4	AGAGAATCTGGTGGCTGTGGAGAC	AAAGGCTTGGGCTTGAATGGAGTC
PI3K	TCTGGAATGTGTGGCTGGAGTTTG	GGAGGAGGAAGCGGTGGTCTATC
AKT	CTCAACAACCTTCTCAGTGGCACAATG	GCAGGCAGCGGATGATGAAGG
p65	GATGGCTTCTATGAGGCTGAACTCTG	CTTGCTCCAGGTCTCGCTTCTTC
GAPDH	GTCCATGCCATCACTGCCACTC	CGCCTGCTTACCACCTTCTTG

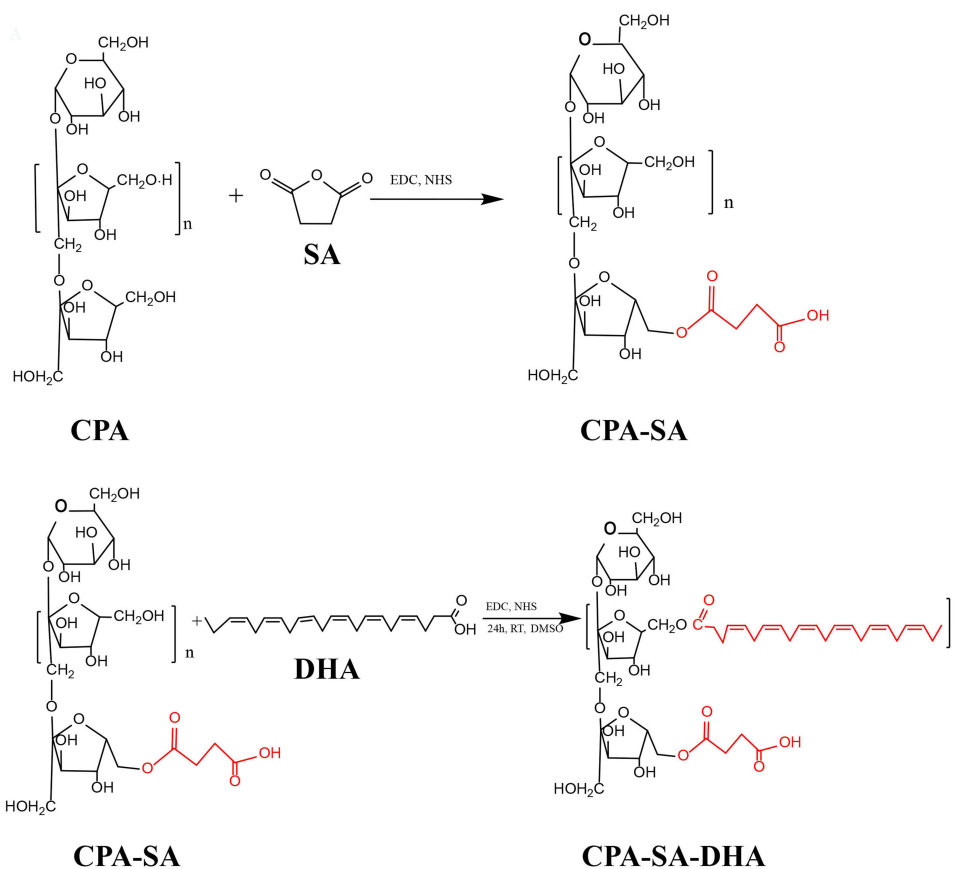


Figure 1 Illustration of the responses of CPA, SA, and DHA to CSD conjugate.

The ^1H NMR spectra of CPA-SA showed characteristic peaks at 2.61 ppm and 3.61 ppm, which correspond to the protons of carbon-carbon bonds ($-\text{CH}_2-\text{CH}_2-$, $-\text{CH}_2-$). The signals at 2.81 ppm and 5.38 ppm in the CSD conjugate spectrum were attributed to the most prominent peaks of DHA protons, confirming that DHA was successfully conjugated to CSD (Figure 2B).

Table 2 Effect of Different Grafting Degrees of SA and DHA on Product State and Yield

Product	Mol ratio	Status	Yield (%)
CPA-SA	1:3	Powdered	29.36%
	1:6	Powdered	25.50%
	1:9	Powdered	23.50%
CPA-DHA	1:1	Powdered	49.30%
	1:3	Oily	
	1:6	Oily	
CPA-SA-DHA	1:3:1	Powdered	18.00%
	1:6:1	Powdered	41.60%
	1:9:1	Powdered	31.30%
	1:3:3	Oily	
	1:6:3	Oily	
	1:9:3	Oily	

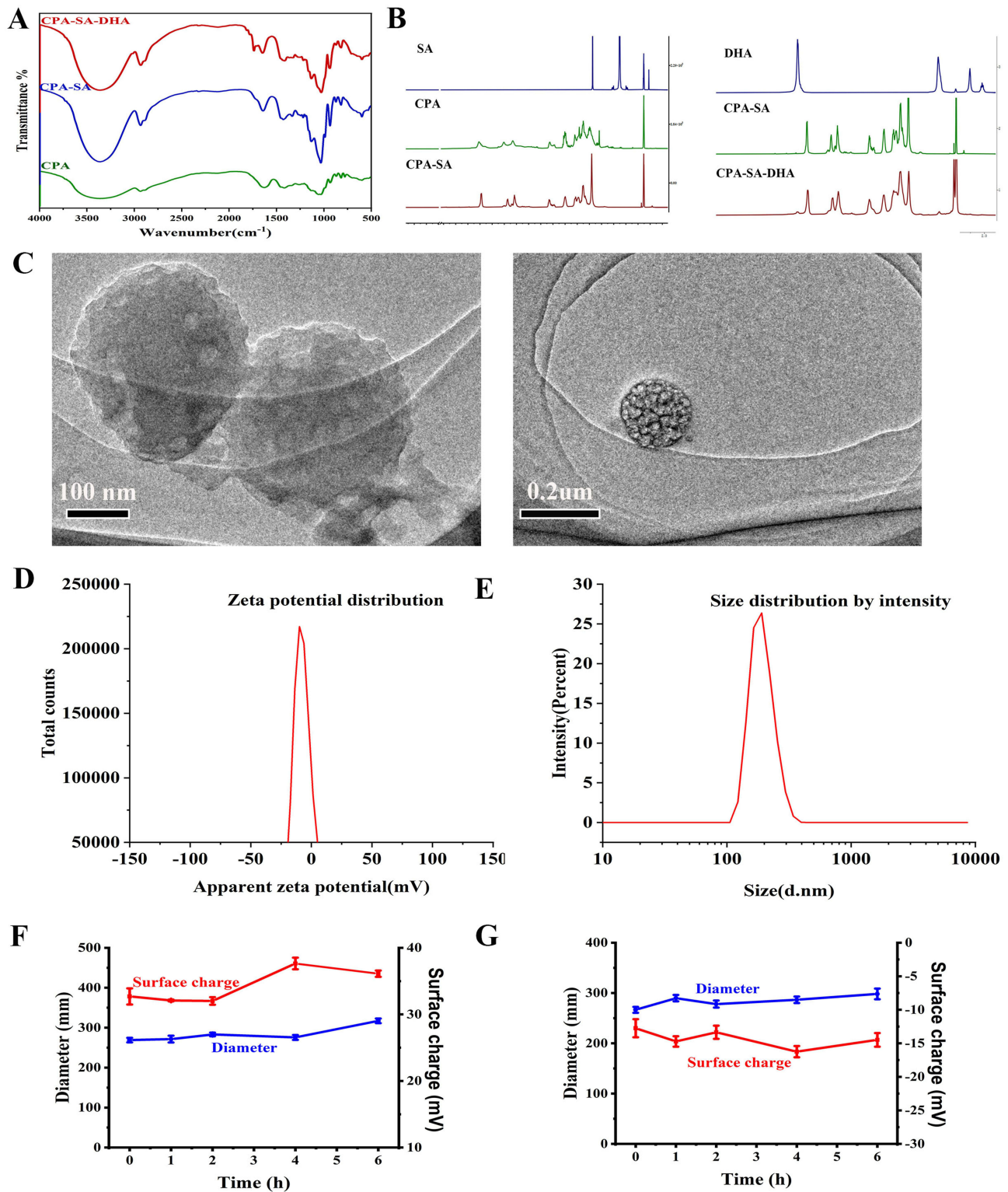


Figure 2 Preparation and characterisation of CSD Nps. (A and B) 1 h NMR spectra and FTIR spectra of different compounds. (C) Representative TEM images of CSD Nps. (D and E) Zeta potential and size distribution of CSD Nps. (F and G) The stability evaluation of CSD Nps in artificial gastric juice and artificial intestinal juice after incubated for various time.

Preparation and Characterisation of CSD Nps Powder

Under the optimized conditions, DLS of the samples revealed that the CSD preparations exhibited an average diameter of 180 ± 23.2 nm. PDI is an index which was used to assess the uniformity of the CSD nanoparticle distribution. A PDI value below 0.3 indicates a uniform distribution. In the case of the developed CSD Nps, the PDI was observed to be 0.230 ± 0.003 . Zeta potential, another characterization parameter, is closely related to the stability of Nps (Table 3). As mentioned before, positively charged proteins tend to accumulate in the inflammatory site of the intestine. Therefore, it is meaningful to develop negatively charged nanoparticles. The results showed that TEM of CSD preparations (Figure 2C) demonstrated that the fabricated nanoparticles had well-defined spherical shapes. Furthermore, the zeta potential of the CSD Nps was -29.8 ± 5.3 mV (Figure 2D and E). Considering the particle size, PDI, and zeta potential, the prepared CSD Nps were found to be suitable for the colitis microenvironment. In addition, the stability of CSD Nps in artificial gastric juice and artificial intestinal juice was assessed. The findings indicated that there was no significant change in the zeta potential and diameter of CSD Nps after being incubated for various durations (0–6 h) (Figure 2F and G).

CSD Assemblies Exhibited Better Anti-Inflammatory Property in LPS Induced Inflammatory NCM460 Cells

The *in vitro* anti-inflammatory properties of CSD Nps were assessed using RT-qPCR. First, we determined the cell viability of CPA, CSD Mix, and CSD Nps at different concentrations using the CCK8 test. The results indicated that CPA exhibited the highest cell viability within the concentration range of 50–3200 $\mu\text{g mL}^{-1}$. In contrast, CSD Mix and CSD Nps demonstrated different levels of cell viability, with CSD Mix showing 60–70% viability and CSD Nps showing 90–120% viability at concentrations of 50–400 $\mu\text{g mL}^{-1}$. This suggests that the addition of SA and DHA decreased cell viability; however, CSD Nps exhibit better cell viability compared to CSD Mix (Figure 3A–C). To establish an inflammatory colitis cell model, various concentrations of LPS were incubated with NCM460 cells. The CCK8 results showed that cell viability decreased as the LPS concentration increased. When the LPS concentration exceeded 30 $\mu\text{g mL}^{-1}$, the IC₅₀ fell below 50% (Figure 3D). We selected IL-6 as an indicator to determine a suitable LPS concentration. Figure 3E shows that 20 $\mu\text{g mL}^{-1}$ LPS significantly increased the IL-6 level, indicating that this concentration is appropriate for inducing inflammation in NCM460 cells.

To determine the protective effect of CPA, CSD Mix, and CSD Nps on LPS-induced inflammatory NCM460 cells, the mRNA level of IL-6, IL-1 β , IFN- γ and TNF- α were analyzed. The results showed that the expression of the inflammatory factors mentioned above was significantly increased in the LPS-treated group. CPA inhibited the level of IL-1 β but had no effect on the levels of IL-6, IFN- γ , and TNF- α . CSD Mix and CSD Nps were able to suppress the mRNA expression levels of IL-6, IL-1 β , and TNF- α to varying degrees (Figure 3F–I). Furthermore, CSD Nps provided better protection than CSD Mix.

The Safety Evaluation of CSD Nps

To evaluate the toxicity and safety of CSD Nps, the formulation was administered to UC mice via intragastric route for two weeks. After that, the mice were sacrificed to collect samples. The results showed that in comparison to the model group, the CSD Nps-treated group did not exhibit any typical pathological changes in the heart, liver, spleen, lung, and kidney (Figure 4A). This suggests that CSD Nps is suitable for use in animal experiments.

CSD Nps Significantly Improved Bioavailability of CPA in UC Mice

Our previous study demonstrated that CPA effectively alleviated mouse colitis symptoms induced by DSS, positioning it as a potential new drug candidate derived from plants.²⁹ To gain further insights into the clinical application of CPA, we

Table 3 Physicochemical Characteristics of CSD NPs

	Particle size (nm)	PDI	Zeta-potential (mV)
CSD Nps	180 ± 23.2 nm	0.230 ± 0.003	-29.8 ± 5.3

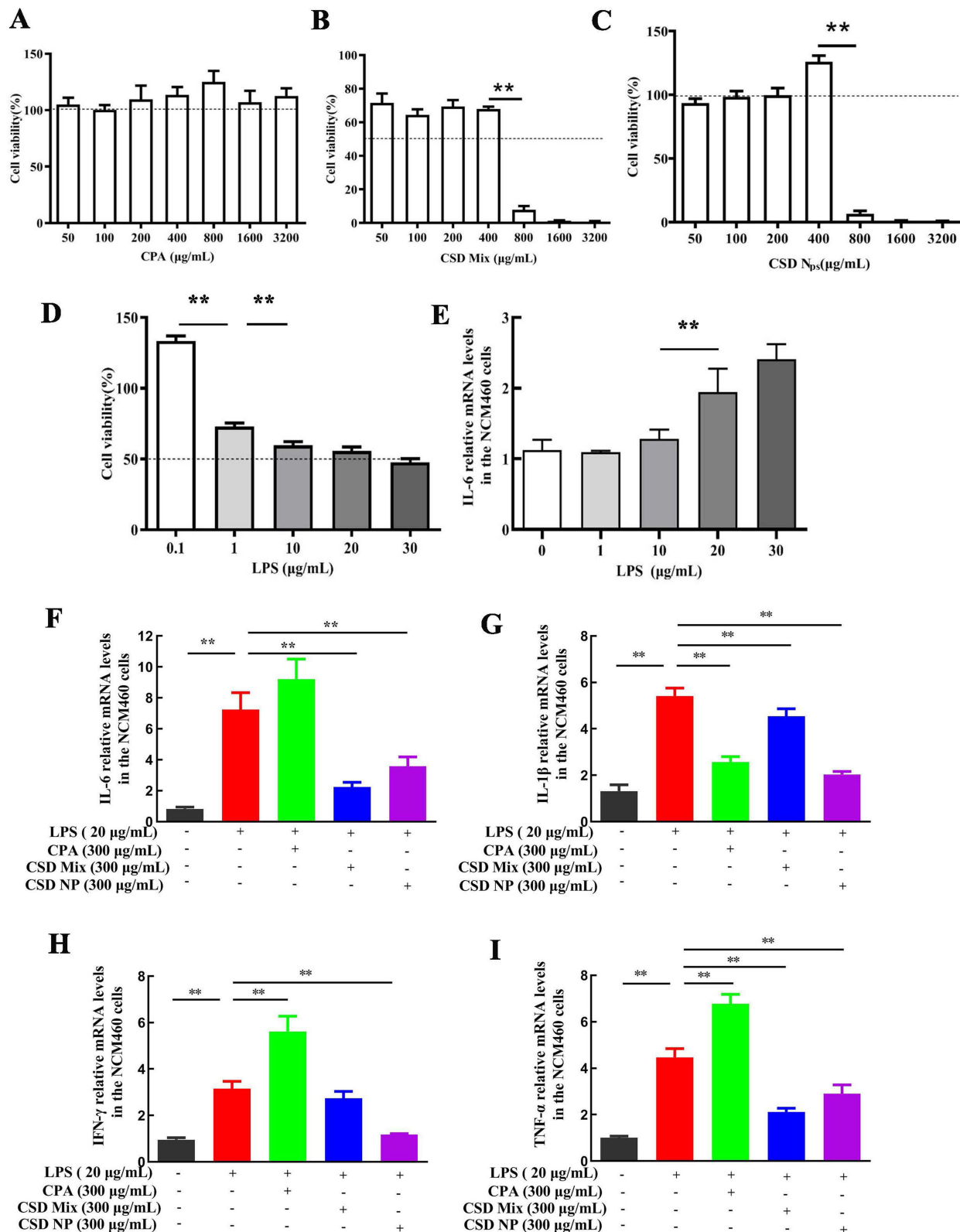


Figure 3 CSD nanoparticles markedly inhibit inflammation-related cytokines in LPS-induced inflammatory NCM 460 cell. **(A-D)** Cell viability of NCM 460 cell treated with CPA, CSD Mix, CSD Nps and LPS for 24 h. **(E)** Relative mRNA expression of IL-6 in NCM 460 cell after treated with different concentrations of LPS. **(F-I)** The contents of inflammation-related cytokines including IL-6, IL-1β, IFN-γ and TNF-α. **p < 0.01 vs DSS group.

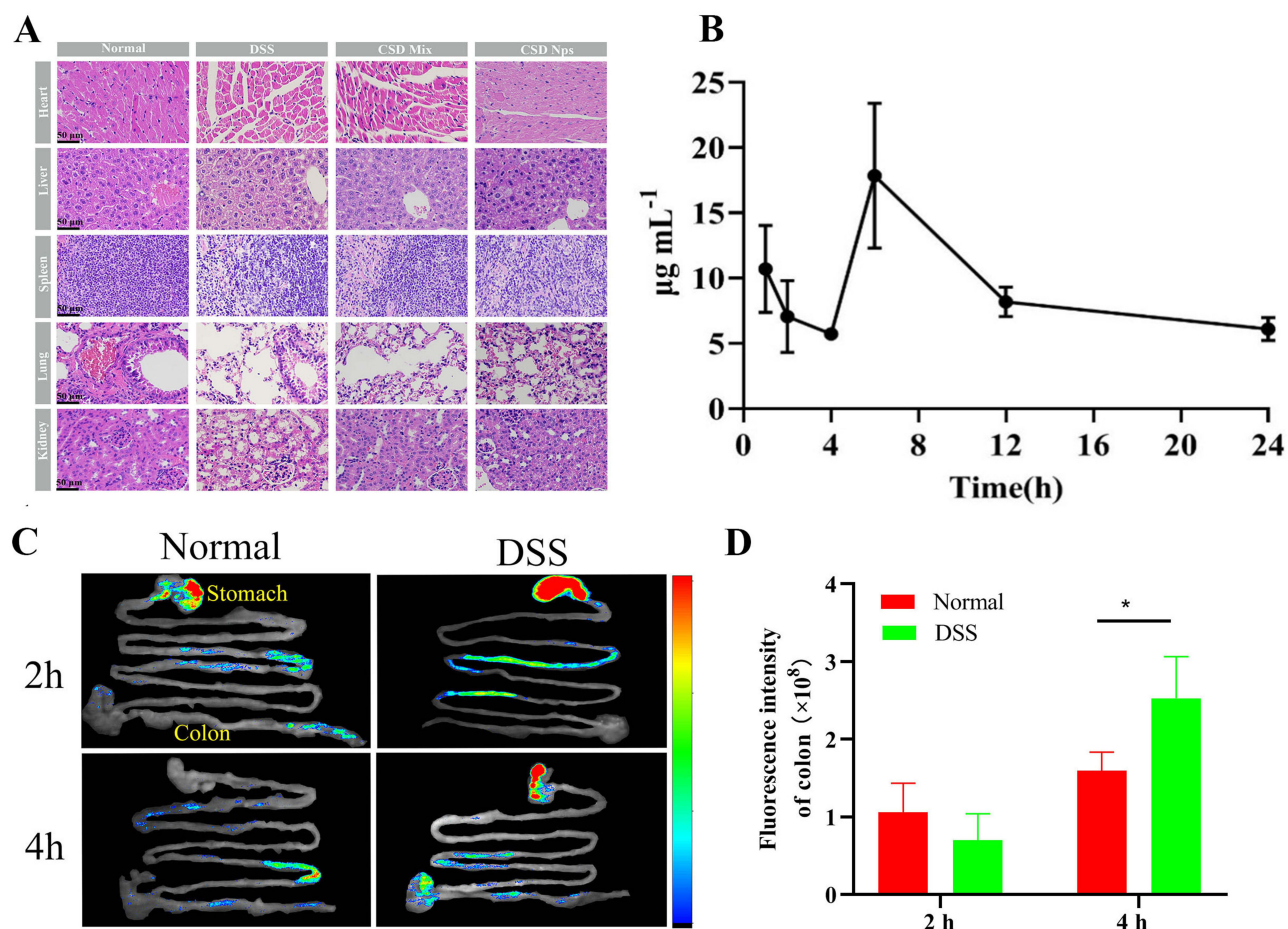


Figure 4 HE staining micrographs of different tissues including heart, liver, spleen, lung, and kidney (A). The mean plasma concentration-time profiles of CSD Nps in UC mice (B). Typical graphs of tissue distribution of CSD Nps in the digestive tract of UC mice and normal mice at 2 and 4 h after oral administration (C). Quantitative analysis of fluorescence intensity in the colon at each time point (D). * $p < 0.05$ vs DSS group.

investigated its pharmacokinetic characteristics. The findings revealed that CPA exhibited low bioavailability and poor oral absorption.¹⁵ Consequently, we developed a new formulation with improved bioavailability. To ascertain whether CSD Nps offers enhanced bioavailability, the pharmacokinetics were evaluated in UC mice. Interestingly, the pharmacokinetic profiles of CSD Nps displayed double peaks, with the first peak occurring at 6 hours (Figure 4B). The half-life ($T_{1/2}$) and mean residence time (MRT) were notably extended to 24.81 ± 6.44 hours and 29.99 ± 5.38 hours, respectively. Moreover, the area under the curve ($AUC_{(0 \rightarrow \infty)}$) significantly increased to $386.83 \pm 61.22 \text{ mg L}^{-1} \text{ h}^{-1}$, indicating a substantial improvement in the bioavailability and circulation time of CSD Nps in UC mice (Table 4). This can be attributed to two factors: firstly, the interaction between the negatively charged nanoparticles and the colon mucosa reduced the excretion of CSD Nps, thereby prolonging their residence time in the colon. Secondly, the oral administration of CSD Nps facilitated the penetration of the entire intestinal mucosa and accumulation in colitis tissues, owing to their suitable particle size of $180 \pm 23.2 \text{ nm}$. Additionally, this particle size also prevented rapid elimination through diarrhea. Consequently, CSD Nps holds promise as a potential therapy for UC.

CSD Nps Has Longer Residence Time in Colon

To investigate the potential prolonged retention time of CSD Nps in the colon, we intragastrically administered 56 mg kg^{-1} FCSD Nps to both normal mice and UC mice. The fluorescence intensity of FCSD Nps in stomach and colon was examined at 2 and 4 h (Figure 4C and D). The results revealed that compared to normal mice, UC mice exhibited greater retention of CSD Nps in the stomach and jejunum at 2 hours. Additionally, UC mice showed increased retention of CSD

Table 4 Pharmacokinetic Parameters of CSD NPs After Oral Administration (n = 6)

Parameter	CSD Nps
$T_{1/2Z}(h)$	24.81 ± 6.44
$AUC_{(0 \rightarrow \infty)} (mg L^{-1} h^{-1})$	386.83 ± 61.22
$CL(L h^{-1} kg^{-1})$	0.15 ± 0.02
$V_d(L kg^{-1})$	4.20 ± 0.38
$MRT_{(0 \rightarrow \infty)}(h)$	29.99 ± 5.38

Nps in the colon at 4 hours, suggesting that CSD Nps had a more favorable effect on colon retention and could be more suitable for treating colitis. This may be due to the negatively charged nature of Nps, which allows them to adhere to positively charged proteins in damaged areas of the intestinal mucosa.

Oral Administration of CSD Nps Attenuates UC

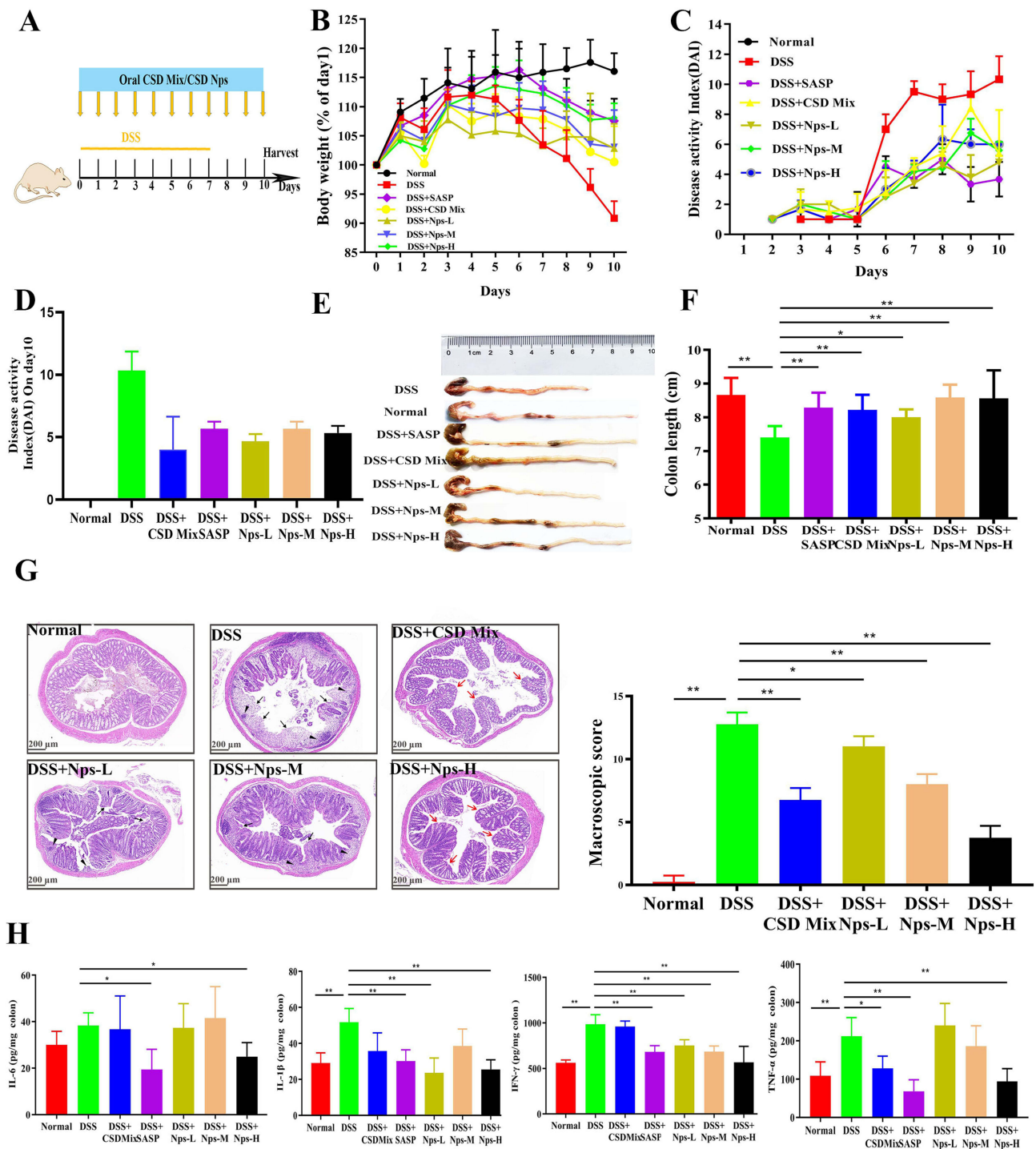
The therapeutic potential of CSD Nps was evaluated in a DSS-induced UC mice model. The UC mice were treated with saline, SASP, CSD Mix, and CSD Nps (28, 56, 112 mg kg⁻¹) by gavage for 10 days (Figure 5A). Initially, we assessed body weight loss, diarrhea, and fecal bleeding. During the experiment, the model group experienced body weight loss from day 5, while CSD Nps-treated mice showed minimal body weight loss, indicating better body weight recovery compared to the CSD Mix at the same dose (Figure 5B). Furthermore, to evaluate the severity of colitis, the DAI score was calculated according to the values of bodyweight, feces, and gross bleeding of the mice (Figure 5D). The results revealed that the colitis group exhibited significantly higher DAI values. However, CSD Nps intervention significantly attenuated the increased DAI scores (Figure 5C and D). Colon shortening is a critical parameter for assessing inflammation severity. The results showed that DSS treatment led to significant colon shortening (Figure 5E and F). In comparison with the DSS group, CSD Nps treatment markedly attenuated colon length shortening in the DSS group. H&E staining was further applied to evaluate the therapeutic potential of CSD Nps. As shown in Figure 5G, the DSS group exhibited severe colitis symptoms, including crypt destruction, intestinal epithelium damage, and inflammatory cell infiltration. However, the other treated groups showed varying degrees of alleviation in pathological changes. These results suggest that CSD Nps exerts excellent anti-inflammatory effects and appears to attenuate DSS-induced UC.

CSD Nps Markedly Inhibit Inflammation in UC Mice

To evaluate the anti-inflammatory effects of CSD Nps on mice with UC, we measured the levels of TNF- α , IFN- γ , IL-6, and IL-1 β in their colon tissues (Figure 5H). The results showed a significant increase in TNF- α , IFN- γ , and IL-1 β levels in DSS-treated mice. Excessive production of inflammatory factors by immune cells is a key characteristic of DSS-induced colitis. Elevated levels of pro-inflammatory cytokines can lead to apoptosis of epithelial cells, disruption of the epithelial barrier, and prolonged disease progression. However, we observed that CSD Mix, CSD Nps, and SASP reversed these changes to some extent. Specifically, the administration of CSD Mix at a high dosage of 112 mg kg⁻¹ resulted in a reduction of TNF- α levels. However, it did not have any effect on the elevated levels of IFN- γ and IL-1 β . On the other hand, CSD Nps could ameliorated the levels of TNF- α , IFN- γ and IL-1 β . These findings suggest that CSD Nps have a more effective protective effect than CSD Mix at the same dose, which was achieved through the regulating cytokine levels in the colon tissue.

CSD Nps Ameliorate Gut Microbiota Imbalance in UC Mice

Multiple studies have shown a close association between gut microbiota and the progression of UC.³ Imbalances in the gut microbial population can stimulate the production of pro-inflammatory cytokines. Conversely, repairing the dysbiosis of gut microbiota could alleviate the imbalance of intestinal homeostasis and inhibit the inflammatory response.³ In this study, 16S rRNA sequencing technology was used to investigate changes in gut microbiota in UC mice. Consistent with other studies, the abundance of gut microbiota was found to be decreased in UC mice.³ However, it was still unknown whether the therapeutic



effect of CSD Nps was related to the composition of gut microbiota. Chao 1 index were used to evaluate the richness and diversity of the gut microbial community. The results showed that the Chao 1 index were significantly decreased in DSS-treated mice, but treatment with CSD Nps effectively reversed the Chao 1 index (Figure 6A). At the phylum and genus levels, the composition of gut microbiota was significantly altered in DSS-treated mice. Compared to normal mice, Bacteroides and

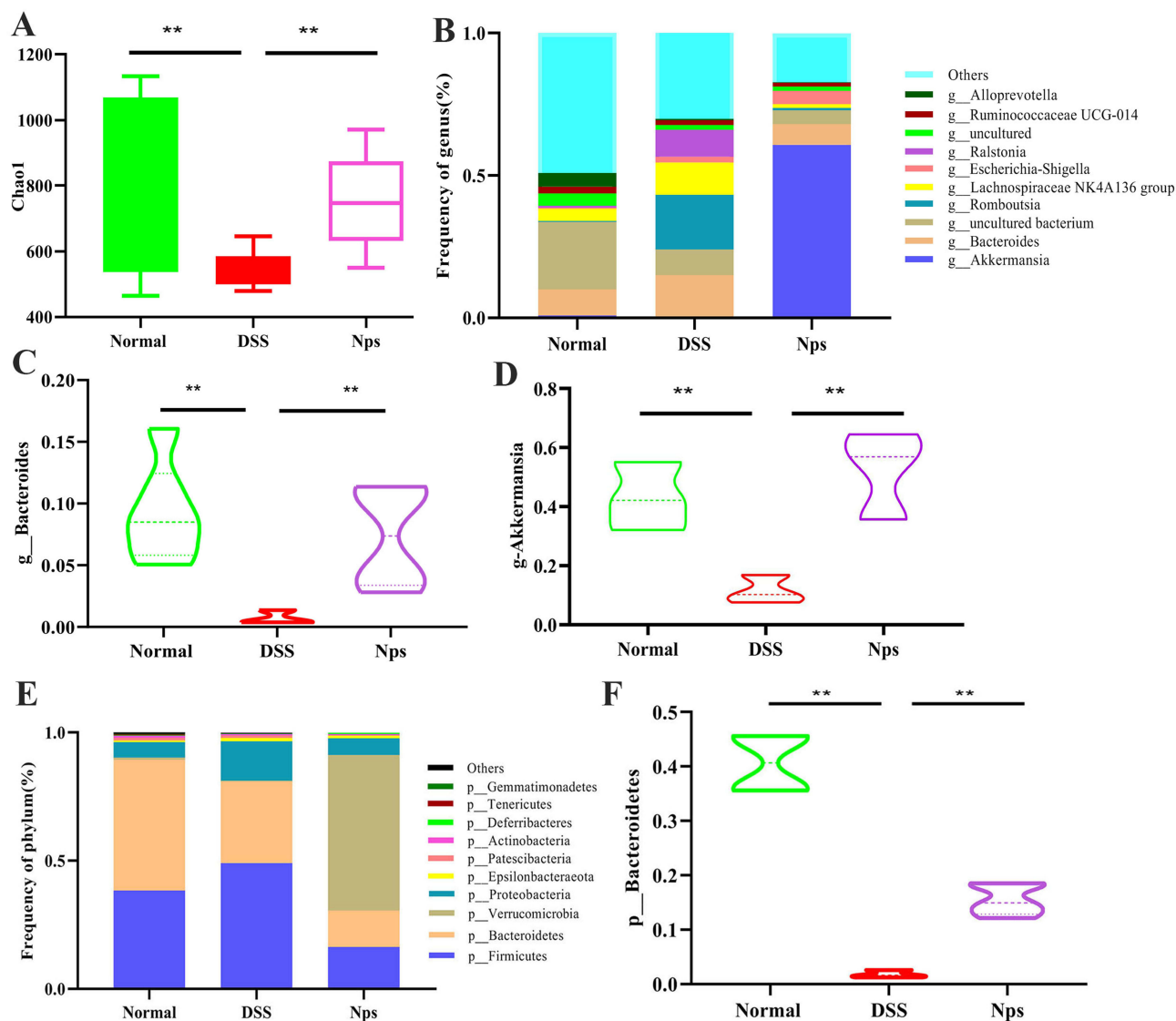


Figure 6 CSD nanoparticle regulated the composition of gut microbiota in UC mice. **(A)** Alpha diversity indexes chao1; **(B)** The histogram of gut microbiota composition at genus horizontal; **(C and D)** The relative abundance of bacteroides and akkermansia; **(E)** The histogram of gut microbiota composition at phylum horizontal; **(F)** The relative abundance of bacteroidetes. ** $p < 0.01$ vs DSS group.

Akkermansia were significantly decreased in UC mice. It has been reported that Akkermansia is reduced in IBD patients with inflammatory bowel diseases, and it is negatively correlated with pro-inflammatory cytokines.³⁰ In this study, CSD Nps intervention reversed the reduction in Akkermansia abundance in DSS-induced colitis mice, suggesting that CSD Nps intervention can inhibit inflammation by restoring gut microbiota composition. Moreover, at the genus level, Bacteroides was also significantly decreased in DSS-treated mice (Figure 6B–F). Bacteroides is recognized as the most common probiotic and has been found to have better anti-inflammatory effects by regulating the production of its metabolites, such as butyric acid and lactic acid.³⁰ These changes were reversed after CSD Nps intervention, indicating that CSD Nps can effectively regulate the structure of gut microbiota.

CSD Nps May Ameliorate Gut Microbiota Imbalance by regulating TLR4/NF- κ B Signaling Pathway in UC Mice

Multiple studies have shown that gut microbiota primarily affects the health of the host through its metabolites, such as saturated fatty acids and inflammatory factors.³⁰ When the gut microbiota is disrupted, increased levels of LPS can be

detected in the serum of UC patients. This can impair gut barrier function and lead to endotoxemia.^{30,31} It has been reported that LPS acts as an agonist of TLR4, and the TLR4/NF- κ B pathway plays a crucial role in the inflammatory response induced by LPS in both in vivo and in vitro settings³¹(Figure 7). Therefore, to further investigate the anti-inflammatory mechanism of CSD Nps in DSS-induced colitis mice, the classical inflammatory signaling pathways TLR4/NF- κ B was investigated. The expression levels of the TLR4/NF- κ B signaling pathway at both the gene and protein levels. As shown in Figure 7, compared to the normal group, the model group exhibited significantly increased mRNA

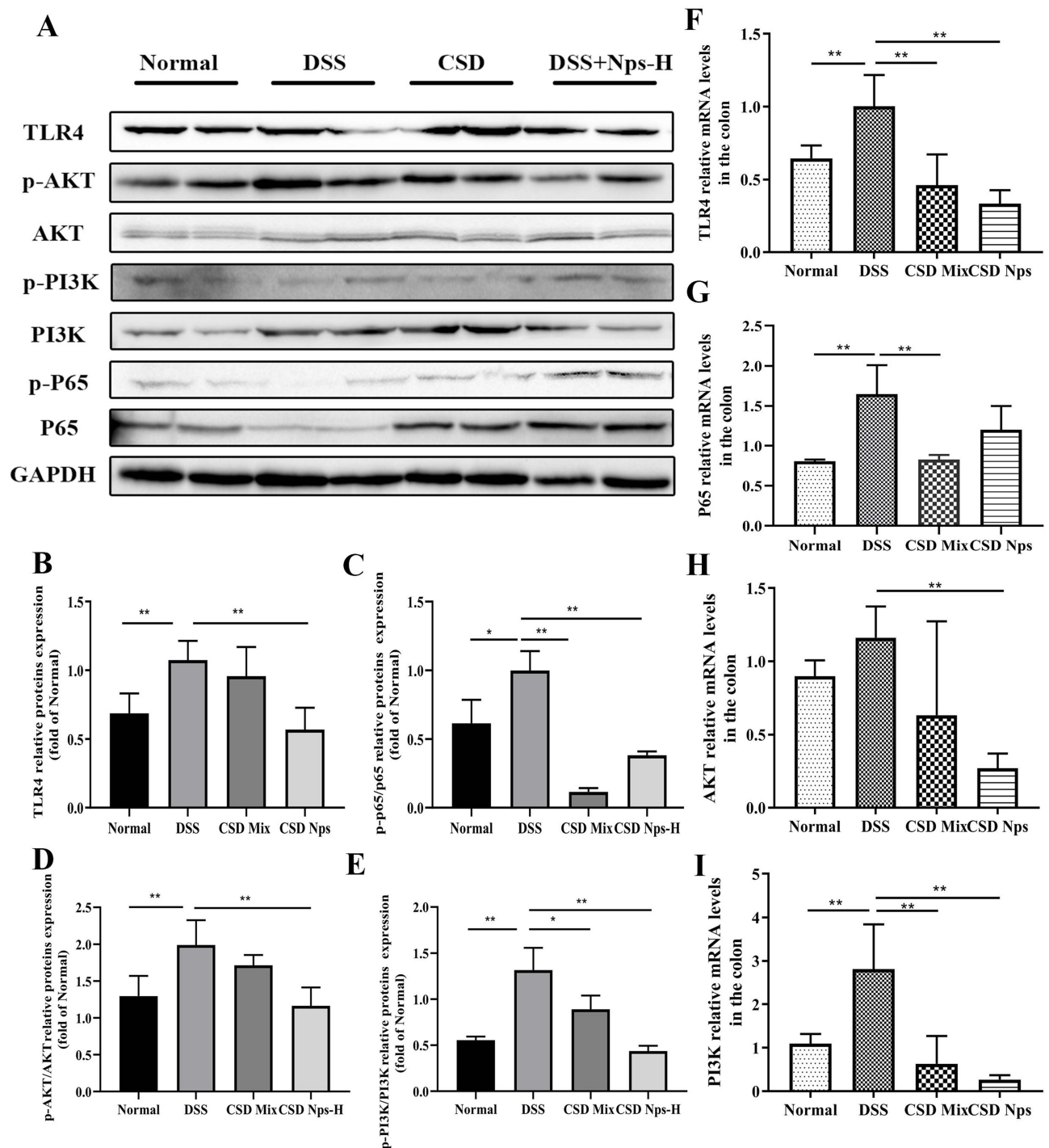


Figure 7 CSD nanoparticles regulated the gene and protein levels of TLR4/NF- κ B signaling pathway in colitis mice. (A-E) Western blot outcomes and histogram analysis of TLR4, PI3K, AKT, P65. (F-I) The mRNA expression level of TLR4, PI3K, AKT, P65. * $p < 0.05$ vs DSS group, ** $p < 0.01$ vs DSS group.

and protein expression of TLR4 and its target genes (AKT, PI3K, and NF- κ B), which aligns with the findings of Cammarota and Masayuki Fukata et al^{32,33}. However, this increase was reversed after intervention with CSD Nps. Therefore, the therapeutic effect of CSD Nps can be partly attributed to the inhibition of the TLR4/NF- κ B inflammatory pathway.

Conclusions

In this study, we investigated a new therapeutic approach for UC by creating negatively charged amphipathic prodrugs called CSD. The self-assembled nanoparticles showed good safety, as determined by examining pathological changes in the heart, liver, spleen, lung, and kidney of mice in the CSD Nps treated group. The nanoparticles were found to stay in the colonic microenvironment for a longer period due to the interaction between positive and negative charges. Compared to CPA, the CSD nanoparticles exhibited better bioavailability in UC mice. They played a protective role against UC by inhibiting the activation of the NF- κ B signaling pathway and regulating the abundance of gut microbiota.

Data Sharing Statement

Data will be made available by the corresponding author Yun-yun Shao upon request.

Funding

This study was supported by Special Fund from Medicinal Basic Research Innovation Center of Chronic Kidney Disease, Ministry of Education, Shanxi Medical University (No.CKD/SXMU-2024-03), Shanxi Basic Research Program (grant:202303021222329) and Youth fund of the second affiliated hospital of Shanxi medical university (grant: 202301-9 and 202301-32).

Disclosure

The authors report no declarations of interest.

References

1. Chen Q, Gou S, Ma P, et al. Oral administration of colitis tissue-accumulating porous nanoparticles for ulcerative colitis therapy. *Int J Pharm.* 2019;557:135–144. doi:10.1016/j.ijpharm.2018.12.046
2. Ruiz PA, Morón B, Becker HM, et al. Titanium dioxide nanoparticles exacerbate DSS-induced colitis: role of the NLRP3 inflammasome. *Gut.* 2017;66(7):1216–1224. doi:10.1136/gutjnl-2015-310297
3. Luo R, Lin M, Fu C, et al. Calcium pectinate and hyaluronic acid modified lactoferrin nanoparticles loaded Rhein with dual-targeting for ulcerative colitis treatment. *Carbohydr Polym.* 2021;263:117998. doi:10.1016/j.carbpol.2021.117998
4. Collnot EM, Ali H, Lehr CM. Nano- and microparticulate drug carriers for targeting of the inflamed intestinal mucosa. *J Controlled Rel.* 2012;161(2):235–246. doi:10.1016/j.jconrel.2012.01.028
5. Liu C, Yan X, Zhang Y, et al. Oral administration of turmeric-derived exosome-like nanovesicles with anti-inflammatory and pro-resolving bioactions for murine colitis therapy. *J Nanobiotechnol.* 2022;20(1):206. doi:10.1186/s12951-022-01421-w
6. Müller EK, Białas N, Epple M, Hilger I. Nanoparticles carrying NF- κ B p65-specific siRNA alleviate colitis in mice by attenuating NF- κ B-related protein expression and pro-inflammatory cellular mediator secretion. *Pharmaceutics.* 2022;14(2):419. doi:10.3390/pharmaceutics14020419
7. Allawadhi P, Singh V, Govindaraj K, et al. Biomedical applications of polysaccharide nanoparticles for chronic inflammatory disorders: focus on rheumatoid arthritis, diabetes and organ fibrosis. *Carbohydr Polym.* 2022;281:118923. doi:10.1016/j.carbpol.2021.118923
8. Du YE, Lee JS, Kim HM, et al. Chemical constituents of the roots of *Codonopsis lanceolata*. *Arch. Pharmacol Res.* 2018;41(11):1082–1091. doi:10.1007/s12272-018-1080-9
9. Gao C, Zhou Y, Chen Z, et al. Turmeric-derived nanovesicles as novel nanobiologics for targeted therapy of ulcerative colitis. *Theranostics.* 2022;12(12):5596–5614. doi:10.7150/thno.73650
10. Wu Z, Zhang Y, Nie G, et al. Tracking the gastrointestinal digestive and metabolic behaviour of *Dendrobium officinale* polysaccharides by fluorescent labelling. *Food Funct.* 2022;13(13):7274–7286. doi:10.1039/d2fo01506d
11. He JY, Zhu S, Komatsu K, Goda Y, Cai SQ. Genetic polymorphism of medicinally-used *Codonopsis* species in an internal transcribed spacer sequence of nuclear ribosomal DNA and its application to authenticate *Codonopsis Radix*. *J Nat Med.* 2014;68(1):112–124. doi:10.1007/s11418-013-0780-1
12. Zou YF, Chen XF, Malterud KE, et al. Structural features and complement fixing activity of polysaccharides from *Codonopsis pilosula* Nannf. var. *modesta* L.T.Shen roots. *Carbohydr Polym.* 2014;113:420–429. doi:10.1016/j.carbpol.2014.07.036
13. Shao YY, Zhao YN, Sun YF, et al. Investigation of the internalization and transport mechanism of *Codonopsis Radix* polysaccharide both in mice and Caco-2 cells. *Int J Biol Macromol.* 2022;215:23–35. doi:10.1016/j.ijbiomac.2022.06.104
14. Zhou J, Wang J, Wang J, et al. An inulin-type fructan CP-A from *Codonopsis pilosula* attenuates experimental colitis in mice by promoting autophagy-mediated inactivation of NLRP3 inflammasome. *Chin J Nat Med.* 2024;22(3):249–264. doi:10.1016/S1875-5364(24)60556-X

15. Guo Y, Shao YY, Zhao YN, et al. Pharmacokinetics, distribution and excretion of inulin-type fructan CPA after oral or intravenous administration to mice. *Food Funct.* 2022;13(7):4130–4141. doi:10.1039/d1fo04327g
16. Yamazaki N, Kojima S, Bovin NV, André S, Gabius S, Gabius HJ. Endogenous lectins as targets for drug delivery. *Adv Drug Delivery Rev.* 2000;43(2–3):225–244. doi:10.1016/s0169-409x(00)00071-5
17. Yan H, Yalagala RS, Yan F. Fluorescently labelled glycans and their applications. *Glycoconjugate J.* 2015;32(8):559–574. doi:10.1007/s10719-015-9611-9
18. Lee Y, Sugihara K, Gilliland MG 3rd, Jon S, Kamada N, Moon JJ. Hyaluronic acid-bilirubin nanomedicine for targeted modulation of dysregulated intestinal barrier, microbiome and immune responses in colitis. *Nature Mater.* 2020;19(1):118–126. doi:10.1038/s41563-019-0462-9
19. Nai J, Zhang C, Shao H, et al. Extraction, structure, pharmacological activities and drug carrier applications of Angelica sinensis polysaccharide. *Int J Biol Macromol.* 2021;183:2337–2353. doi:10.1016/j.ijbiomac.2021.05.213
20. Dou YX, Zhou JT, Wang TT, et al. Self-nanoemulsifying drug delivery system of bruceine D: a new approach for anti-ulcerative colitis. *Int J Nanomed.* 2018;13:5887–5907. doi:10.2147/ijn.S174146
21. Xu H, Luo R, Dong L, et al. pH/ROS dual-sensitive and chondroitin sulfate wrapped poly (β -amino ester)-SA-PAPE copolymer nanoparticles for macrophage-targeted oral therapy for ulcerative colitis. *Nanomedicine.* 2022;39:102461. doi:10.1016/j.nano.2021.102461
22. Watanabe A, Tanaka H, Sakurai Y, et al. Effect of particle size on their accumulation in an inflammatory lesion in a dextran sulfate sodium (DSS)-induced colitis model. *Int J Pharm.* 2016;509(1–2):118–122. doi:10.1016/j.ijpharm.2016.05.043
23. Liu P, Gao C, Chen H, et al. Receptor-mediated targeted drug delivery systems for treatment of inflammatory bowel disease: opportunities and emerging strategies. *Acta pharmaceutica Sinica B.* 2021;11(9):2798–2818. doi:10.1016/j.apsb.2020.11.003
24. Wu Z, Huang S, Li T, et al. Gut microbiota from green tea polyphenol-dosed mice improves intestinal epithelial homeostasis and ameliorates experimental colitis. *Microbiome.* 2021;9(1):184. doi:10.1186/s40168-021-01115-9
25. Bian X, Wu W, Yang L, et al. Administration of akkermansia muciniphila ameliorates dextran sulfate sodium-induced ulcerative colitis in mice. *Front Microbiol.* 2019;10:2259. doi:10.3389/fmicb.2019.02259
26. Li J, Wang T, Zhu Z, Yang F, Cao L, Gao J Structure features and anti-gastric ulcer effects of inulin-type fructan CP-A from the roots of *Codonopsis Pilosula* (Franch.) Nannf. *Molecules.* 2017; 22: 12. doi:10.3390/molecules22122258.
27. Wang K, Cheng F, Pan X, et al. Investigation of the transport and absorption of Angelica sinensis polysaccharide through gastrointestinal tract both in vitro and in vivo. *Drug Delivery.* 2017;24(1):1360–1371. doi:10.1080/10717544.2017.1375576
28. Yu B, Tang C, Yin C. Enhanced antitumor efficacy of folate modified amphiphilic nanoparticles through co-delivery of chemotherapeutic drugs and genes. *Biomaterials.* 2014;35(24):6369–6378. doi:10.1016/j.biomaterials.2014.04.095
29. Li G, Ju Y, Wen Y, et al. Screening of *Codonopsis Radix* polysaccharides with different molecular weights and evaluation of their immunomodulatory activity in vitro and in vivo. *Molecules.* 2022;27(17). doi:10.3390/molecules27175454
30. Guo C, Guo D, Fang L, et al. Ganoderma lucidum polysaccharide modulates gut microbiota and immune cell function to inhibit inflammation and tumorigenesis in colon. *Carbohydr Polym.* 2021;267:118231. doi:10.1016/j.carbpol.2021.118231
31. Fang S, Wang T, Li Y, et al. Gardenia jasminoides Ellis polysaccharide ameliorates cholestatic liver injury by alleviating gut microbiota dysbiosis and inhibiting the TLR4/NF- κ B signaling pathway. *Int J Biol Macromol.* 2022;205:23–36. doi:10.1016/j.ijbiomac.2022.02.056
32. Fukata M, Chen A, Vamadevan AS, et al. Toll-like receptor-4 promotes the development of colitis-associated colorectal tumors. *Gastroenterology.* 2007;133(6):1869–1881. doi:10.1053/j.gastro.2007.09.008
33. Cammarota R, Bertolini V, Pennesi G, et al. The tumor microenvironment of colorectal cancer: stromal TLR-4 expression as a potential prognostic marker. *J Transl Med.* 2010;8:112. doi:10.1186/1479-5876-8-112

International Journal of Nanomedicine

Dovepress

Publish your work in this journal

The International Journal of Nanomedicine is an international, peer-reviewed journal focusing on the application of nanotechnology in diagnostics, therapeutics, and drug delivery systems throughout the biomedical field. This journal is indexed on PubMed Central, MedLine, CAS, SciSearch[®], Current Contents[®]/Clinical Medicine, Journal Citation Reports/Science Edition, EMBASE, Scopus and the Elsevier Bibliographic databases. The manuscript management system is completely online and includes a very quick and fair peer-review system, which is all easy to use. Visit <http://www.dovepress.com/testimonials.php> to read real quotes from published authors.

Submit your manuscript here: <https://www.dovepress.com/international-journal-of-nanomedicine-journal>